PROCEEDINGS OF SCIENCE

Jet substructure in p+p and p+Au collisions at $\sqrt{s_{\mathrm{NN}}}$ = 200 GeV at STAR

Isaac Mooney for the STAR Collaboration[a,*]

[a] *Wayne State University,*
666 W. Hancock St., Detroit, USA

E-mail: fs3383@wayne.edu

In order to attribute the partonic energy loss experienced by jets (jet quenching) observed in A+A collisions to the traversal of partons through the hot QCD medium, it is necessary to examine the cold nuclear matter (CNM) effects on the corresponding jets. Such an examination has historically been done using p+A collisions. We present fully corrected measurements of the jet mass and SoftDrop groomed jet mass in p+p and p+Au collisions at STAR at $\sqrt{s_{\mathrm{NN}}}$ = 200 GeV as a function of the event activity (EA) to increase or decrease the magnitude of CNM effects. EA is determined in the backward (Au-going) rapidity ($-5.0 < \eta < -3.3$) by the STAR Beam-Beam Counter to minimize auto-correlation with jets measured at mid-rapidity. Comparison of the jet mass distribution in p+Au collisions to that in p+p collisions allows for isolation of CNM effects in anticipation of an upcoming jet mass measurement in Au+Au collisions.

HardProbes2020
1-6 June 2020
Austin, Texas

*Speaker

1. Introduction

As hard partons from high-Q^2 scatterings evolve in vacuum, they radiate stochastically and fragment into hadrons which lend the resulting jet a unique substructure. Studying jet substructure gives insight into various aspects of QCD, from the initial hard scattering, to the parton shower, and eventual hadronization. Jet mass, M, is one such substructure observable, belonging to a generic class of angularity observables [1], defined as the magnitude of the four-momentum sum of constituents ($M = |\sum_{i\in J} p_i| = \sqrt{E^2 - \mathbf{p}^2}$). The mass of a reconstructed jet is a proxy for the initial parton's virtuality [2]. Measurements of the jet mass are expected to provide vital inputs to Monte Carlo (MC) models' implementations of parton shower and hadronization algorithms. In addition, to focus on the perturbative parton shower, we suppress wide-angle non-perturbative (soft) radiation with SoftDrop grooming [7] and report both groomed and ungroomed jet mass.

In 2016, the PHENIX collaboration reported an unexpected jet production enhancement (suppression) in peripheral (central) p+Au collisions compared to p+p collisions [3]. Studying jet substructure in p+Au collisions will help determine whether this effect is due to jet modification in a cold nuclear medium. Addressing this question is necessary for interpreting measurements of jet mass in a hot nuclear medium.

2. Measurement

This study utilizes STAR data for proton-proton collisions at $\sqrt{s} = 200\,\text{GeV}$ from 2012 and proton-gold collisions at $\sqrt{s_{\text{NN}}} = 200\,\text{GeV}$ from 2015. For both collision systems, we require a jet patch trigger (see [4]) and reconstruct jets from charged tracks in the time projection chamber (TPC) and energy deposits in the barrel electromagnetic calorimeter (BEMC) using the anti-k_{T} algorithm with a jet resolution parameter $R = 0.4$. Event, track, tower, and jet selections are the same as in [4] but for one additional selection: we require jet mass above $1\,\text{GeV}/c^2$, due to poor detector resolution below this. We report jets with transverse momentum (p_{T}) between 20 and $45\,\text{GeV}/c$.

To correct for detector effects such as tracking efficiency and momentum resolution, we perform a two-dimensional (M, p_{T}) iterative Bayesian unfolding implemented in the RooUnfold package [5]. In the case of p+p collisions, we construct a response matrix with particle-level events simulated by PYTHIA-6.4.28 Perugia 2012 (a STAR tune) [6] and detector-level events simulated by the PYTHIA events run through a GEANT-3 STAR detector simulation, and embedded in p+p zero-bias events as an estimate of background. In p+Au collisions, we use the same particle-level events, but embed these detector-level events further into a p+Au minimum-bias background.

Systematic uncertainties are made up of four main components: a tracking efficiency uncertainty of 4%; a tower gain uncertainty of 3.8%; a hadronic correction variation from the nominal 100% subtraction of matched tracks' momenta from tower energy to 50%; and uncertainties on the unfolding procedure such as variation in iteration parameter and the shape of the priors. Uncertainty in background estimation for p+Au unfolding is also considered.

For p+Au collisions, the event activity (EA) is determined by deposited energy in STAR's backward ($-5 < \eta < -3.4$) inner Beam-Beam Counter (iBBC) on the Au-going side of the detector. In this work, we compare p+Au events with 0-50% EA (high-EA) and 50-100% EA (low-EA). These wide ranges will be refined in future work.

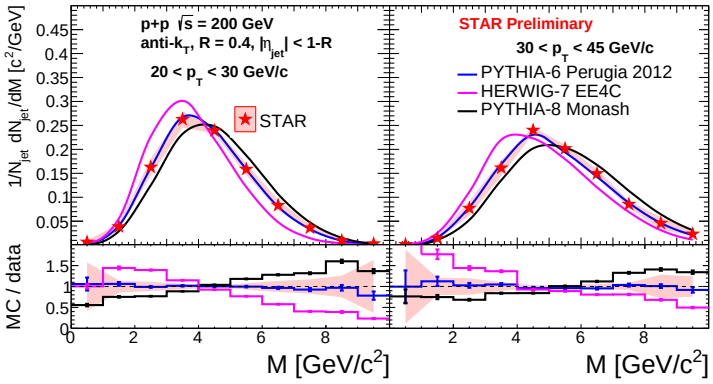

Figure 1: Measurement of the ungroomed jet mass, M, of anti-k_{T} jets in p+p collisions at $\sqrt{s} = 200\,\mathrm{GeV}$ for two jet p_{T} ranges: $20 < p_{\mathrm{T}} < 30\,\mathrm{GeV}/c$ (left), and $30 < p_{\mathrm{T}} < 45\,\mathrm{GeV}/c$ (right). The fully corrected data (with red shaded band denoting systematic uncertainties) are shown in solid red star markers. We compare via ratio to PYTHIA-6 (Perugia 2012 Tune, solid blue line), PYTHIA-8 (Monash Tune, solid black line), and HERWIG-7 (EE4C Tune, solid magenta line) predictions. In the lower panels the relative systematic uncertainty is drawn. Statistical uncertainties are smaller than the size of the marker in all figures.

3. Results

The fully corrected jet mass is shown for p+p collisions in Fig. 1 for $R = 0.4$ jets with $20 < p_{\mathrm{T}} < 30\,\mathrm{GeV}/c$ (left) and $30 < p_{\mathrm{T}} < 45\,\mathrm{GeV}/c$ (right). As the jet p_{T} increases, we observe an increase in the mean jet mass, as expected from pQCD, as well as a broadening of the distribution due to the increase in the available phase space. We also compare the results to three leading-order (LO) MC models: PYTHIA-6 with Perugia 2012 tune, PYTHIA-8 with Monash tune, and HERWIG-7 with EE4C tune, where the latter two are tuned to LHC data. Relevant differences between PYTHIA and HERWIG lie in the shower and hadronization mechanisms, with PYTHIA using a p_{T}-ordered shower and string fragmentation, while HERWIG utilizes an angular-ordered shower and cluster hadronization. We note that PYTHIA-6 describes the data well within systematic uncertainties, while the HERWIG-7 and PYTHIA-8 prefer lower and higher mass jets, respectively.

Next, in order to remove jet constituents arising from soft radiation, we apply the SoftDrop grooming algorithm in tagging mode with $z_{\mathrm{cut}} = 0.1$, $\beta = 0$. We report the groomed mass (M_{g}) in Fig. 2 for ranges of the corresponding *ungroomed* jet p_{T} to allow direct comparison to the ungroomed jet mass. Note that $\langle M_{\mathrm{g}} \rangle$ is reduced (*cf.* Fig. 1) due to the suppression of non-perturbative effects. As before, we compare data (red star markers) to the three LO MC models (solid lines) mentioned above, in the ratio panel. Here we see a reduced systematic uncertainty on the groomed jet mass. The trends are similar to the ungroomed jet mass although disagreement between data and the two LHC-tuned MC models (HERWIG-7 and PYTHIA-8) is reduced.

Figure 3 shows the comparison of the fully corrected jet mass (left) and groomed jet mass (right) in low-EA p+Au collisions (blue stars) to p+p collisions (black stars) for jets with $20 < p_{\mathrm{T}} < 30\,\mathrm{GeV}/c$. We observe no significant difference between them, which is expected.

In Fig. 4, we compare the fully corrected jet mass in low-EA p+Au collisions (blue stars) to high-

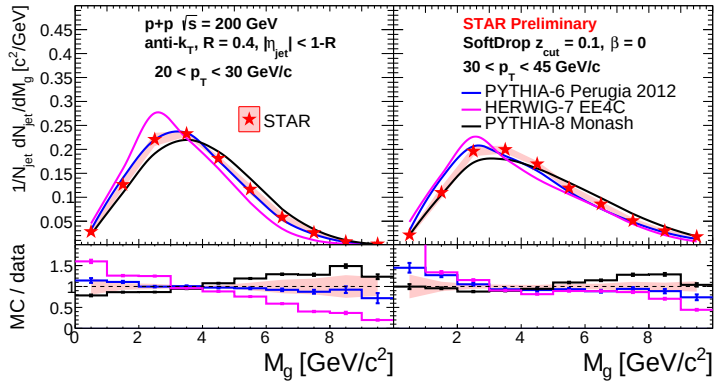

Figure 2: Measurement of the groomed mass, M_{g}, of anti-k_{T} jets in p+p collisions at $\sqrt{s} = 200\,\mathrm{GeV}$. See Fig. 1 for a description of the curves.

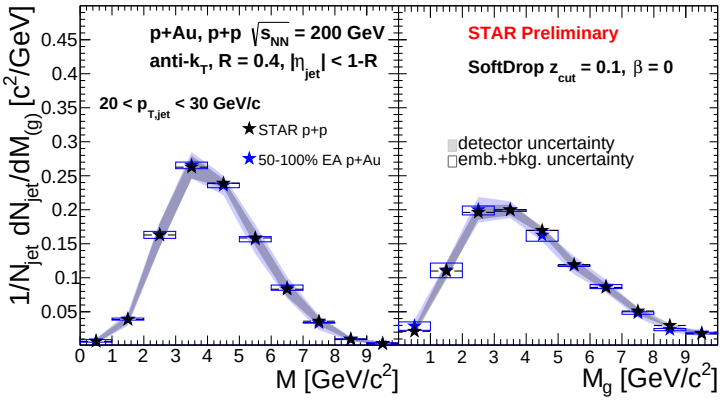

Figure 3: Measurements of jet mass, M (left), and groomed jet mass, M_{g} (right), in low event activity p+Au collisions (blue stars), compared to those in p+p collisions (black stars) as shown in Fig. 1 for a single jet p_{T} selection, $20 < p_{\mathrm{T}} < 30\,\mathrm{GeV}/c$. See § 2 for a definition of event activity. The shaded bands denote the uncertainties that are common between the p+Au and p+p analyses, while the boxes denote the additional embedding and background uncertainty assessed for the p+Au data.

EA p+Au collisions (red stars). The jet mass between the two is consistent within uncertainties, suggesting that the jet structure is unmodified by cold nuclear matter effects in high-EA p+Au collisions. Additionally, the groomed jet mass exhibits similar behavior, indicating that the core of the jets is unmodified as well.

4. Conclusions

We have presented the first fully corrected inclusive jet mass measurements in p+p and p+Au collisions at STAR. The p+p jet mass measurements present an opportunity for further Monte Carlo tuning, while the p+Au jet mass measurement indicates that jet substructure is not significantly

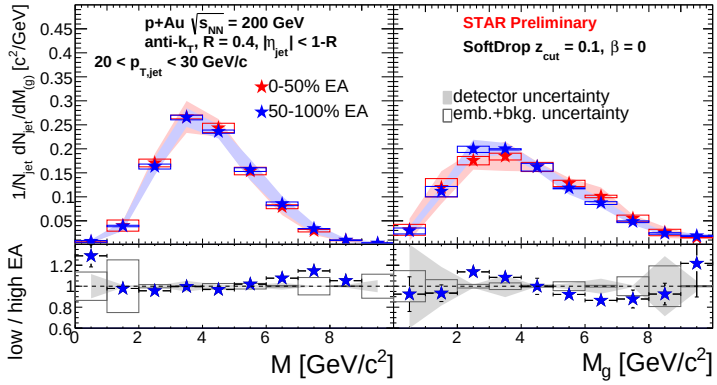

Figure 4: Measurements of ungroomed jet mass, M (left), and groomed jet mass, M_g (right), in high-EA p+Au collisions (red stars), compared to low-EA p+Au collisions (blue stars) as shown in Fig. 3 for a single jet p_T selection, $20 < p_T < 30\,\mathrm{GeV}/c$. See § 2 for a definition of event activity. The ratio between the two event activity classes is shown in the bottom panel. See Fig. 3 for more details on the curves.

affected by CNM effects. It is possible that competing effects on the angular and momentum scales of the jet are cancelled in the mass, so we will investigate the groomed jet momentum fraction, z_g, and radius, R_g, for a full suite of jet substructure observables in p+Au collisions. Additionally, jet resolution parameter dependence will be investigated, and event activity selections narrowed to enhance potential cold nuclear matter effects on the jet mass. Finally, we will use this measurement as a baseline for a similar measurement in the hot nuclear environment of Au+Au collisions.

References

[1] Z.-B. Kang, K. Lee, F. Ringer, *Jet angularity measurements for single inclusive jet production*, JHEP 04 (2018)

[2] A. Majumder, J. Putschke, *Mass depletion: a new parameter for quantitative jet modification*, PRC 93 5

[3] A. Adare et al., *Centrality-dependent modification of jet-production rates in deuteron-gold collisions at* $\sqrt{s_{NN}} = 200\,\mathrm{GeV}$, PRL 116 12

[4] J. Adam et al., *Measurement of groomed jet substructure observables in p+p collisions at* $\sqrt{s_{NN}} = 200\,\mathrm{GeV}$ *with STAR*, arXiv:2003.02114

[5] T. Adye et al., hepunx.rl.ac.uk/~adye/software/unfold/RooUnfold.html

[6] J. Adam et al., *Longitudinal double-spin asymmetry for inclusive jet and dijet production in pp collisions at* $\sqrt{s} = 510\,\mathrm{GeV}$, PRD 100 5

[7] A. J. Larkoski, S. Marzani, G. Soyez, J. Thaler, *Soft Drop*, JHEP 05 (2014)